Available online at www.sciencedirect.com

SciVerse ScienceDirect

Ceramics International 38 (2012) 2139–2144

CERAMICS INTERNATIONAL

www.elsevier.com/locate/ceramint

Crystal structure and mixed ionic–electronic conductivity of $La_{1-x}Ca_xMnO_3$ ($0 \leq x \leq 0.8$) produced by mechanosynthesis

F. Sánchez-De Jesús [a,*], C.A. Cortés-Escobedo [b], A.M. Bolarín-Miró [a], A. Lira-Hernández [a], G. Torres-Villaseñor [c]

[a] Universidad Autónoma del Estado de Hidalgo-AACTyM, Carr. Pachuca -Tulancingo, Km. 4.5, Pachuca 42184, Hidalgo, México
[b] Centro de Investigación e Innovación Tecnológica del IPN, Cda. Cecati S/N, Col. Sta. Catarina, Azcapotzalco, 02250 México D.F., México
[c] Instituto de Investigaciones en Materiales-UNAM, Apdo. Postal 70-360, 04510 México D.F., Mexico

Received 26 May 2011; received in revised form 18 October 2011; accepted 20 October 2011
Available online 25 October 2011

Abstract

The aim of this work was to study the relationship between the crystalline structure, the mixed ionic–electronic conductivity and the calcium content in calcium-doped lanthanum manganites (CLM, $La_{1-x}Ca_xMnO_3$) synthesized by reactive ball milling. Mechanosynthesis was employed to produce nanocrystalline CLM with varying calcium content (x = 0–0.8 in increments of 0.1). Powders of Mn_2O_3, La_2O_3 and CaO mixed in the stoichiometric ratio were used as raw materials. The mechanosynthesis was carried out using a high-energy shaker mixer/mill. X-ray powder diffraction and Rietveld refinement were used to determine the crystalline structure as a function of calcium content. The four-point probe resistivity test was used to measure the electrical resistivity of the compacted and sintered powders using a DC milli-ohm meter. The results showed that the substitution of the La^{3+} ion by the Ca^{2+} ion during mechanosynthesis only changed the lattice parameters but not the orthorhombic *Pnma* structure. The mixed ionic–electronic conductivity increased with the Ca^{2+} content. The best conductivity was observed for the composition of $La_{0.2}Ca_{0.8}MnO_3$.

Keywords: Lanthanum manganites; Mechanosynthesis; Crystal structure; X-ray diffraction; Mixed ionic–electronic conductivity

1. Introduction

Manganites such as $REMnO_3$ (RE = rare earth) have been the subject of recent research due to their magnetic and electrical–electronic properties [1] along with their great potential for use in a wide range of applications including sensors, permanent magnets, catalysts and pigments [1–4]. These properties have also been the reason for research regarding their giant magnetoresistance (GMR) [5–8] and their use as electrode materials for solid-oxide fuel cells (SOFC) [9,10]. Such manganites have very good mixed conductivity and magnetic properties if the REs are partially substituted by alkaline earth atoms with similar ionic radii and different oxidation numbers than the RE in A sites [11–14]. They are capable of forming vacancies that, with other intrinsic and extrinsic defects, give rise to very high electronic and ionic flow and generate magnetic fields. The magnetic and electrical properties are not only closely related to the crystalline structure and stoichiometry of the manganites but also to their defect formation and electronic–ionic flow. Therefore, these materials are mainly used in electronic and microelectronic devices [15–17]. To obtain doped manganites, several synthetic methods have been developed [18–24]. The mechanochemical process (MCP) is an effective, economical and versatile way to produce CLMs using powder oxide mixtures [25–27]. Recently, the high-energy ball milling technique was proven effective in the mechanosynthesis of nanostructured manganites from oxides through a mechanical activation [2,27–29].

Zhang and Saito [30] successfully synthesized $LaMnO_3$ by grinding the mixture of La_2O_3, MnO_2 and Mn_2O_3 powders at room temperature using a high-energy ball mill. The physical and chemical properties of $La_{1-x}Sr_xMnO_3$ were reportedly dependent on the values of x.

* Corresponding author. Tel.: +52 771 7172000; fax: +52 771 71 72133.
E-mail addresses: anabolarin@msn.com, fsanchez@uaeh.edu.mx (F. Sánchez-De Jesús).

0272-8842/$36.00
doi:10.1016/j.ceramint.2011.10.055

The aim of this work was to establish the relationship between the calcium concentration, the crystalline structure and the mixed ionic–electronic conductivity in the CLM powder synthesized by high-energy ball milling and the possibility of using this material as a SOFC cathode.

2. Materials and methods

Five grams of a mixture of Mn_2O_3 (Sigma Aldrich, 99% purity, 5 μm particle size), La_2O_3 (Sigma Aldrich, >99.9% purity, 7 μm particle size) and CaO (Sigma Aldrich, >99.9% purity, 9 μm particle size) powders was used as raw material. The powders were mixed in a stoichiometric ratio according to Eq. (1) with the x values ranging from 0 to 0.8 in increments of 0.1, as reported in previous work [29].

$$0.5Mn_2O_3 + 0.5(1-x)La_2O_3 + xCaO + 0.25xO_2 \rightarrow Ca_xLa_{1-x}MnO_3 \quad (1)$$

The mixture was placed in a steel vial with a volume of 6×10^{-5} m^3 that contained steel balls with a diameter of 0.0127 m. The ball-to-powder weight ratio was 10:1 and ball milling was performed in air. The vial was sealed and shaken in a SPEX 8000D shaker mixer/mill without any control agent for the mechanical energy to initiate the chemical reactions. The powders were milled for 270 min according to the procedure used in previous works [27,28].

The milled powders were characterized at room temperature using a Rigaku D-MAX 2100 diffractometer with a 2θ range of 20–70° at an increment of 0.02° and a 5° angle of incidence. A Cobalt-Kα (λ = 1.7889 Å) target was used. Rietveld refinement was performed on all X-ray patterns using MAUD software [31] to determine the crystal structure and lattice parameters as a function of the milling time.

The milled powder was compacted at 400 MPa by uniaxial pressing to obtain cylindrical test specimens that were 15 mm in diameter and 3 mm in height. The specimens were subsequently sintered in air at 1400 °C for 2 h. The four-point probe resistivity test was used to measure the electrical resistance of the sintered compacts from room temperature to 1413 K; the test was performed using a GW Instek milli-ohm-meter (model GOM-802) with platinum contacts. The total conductivity was reported, which included both the ionic and the electronic conductivities [32].

3. Results and discussion

Table 1 shows the lattice parameters and interplanar distances of the (2 0 0) diffraction plane of the CLM. The specimens with x from 0.1 to 0.8 were milled for 270 min and the lattice parameter a was seen to vary with the Ca^{2+} content. A modification in lattice parameter a was observed when Ca^{2+} was introduced to the $LaMnO_3$ structure by mechanosynthesis, especially between $x = 0.7$ and 0.8. Nevertheless, the three lattice parameters of the structure between $x = 0$ and 0.8 slightly decreased in the same order of magnitude. In addition, the structure maintained the same orthorhombic *Pnma* unit cell in the transition from $LaMnO_3$ ($x = 0.0$) to $La_{0.2}Ca_{0.8}MnO_3$ ($x = 0.8$). The substitution of Ca^{2+} at the positions originally occupied by La^{+3} changed the cell parameters due to the different ionic radii between Ca^{2+} (with an ionic radius of 0.99 Å) and La^{3+} (with an ionic radius of 1.06 Å).

Table 1
Lattice parameter and interplanar distances of the (2 0 0) diffraction plane of the $La_{1-x}Ca_xMnO_3$, for x from 0 to 0.8, milled for 270 min.

Diffraction plane		Lattice parameters (A)			c/a
Ca content (x)	$d_{(2\,0\,0)}$ (nm)	a	b	c	
0.1	2.7649	5.5183	7.7203	5.5643	1.008
0.2	2.7511	5.5133	7.7395	5.5304	1.003
0.3	2.7411	5.4862	7.7243	5.5197	1.006
0.4	2.7318	5.4482	7.6877	5.5225	1.013
0.5	2.7178	5.4750	7.6563	5.4963	1.0038
0.6	2.7097	5.4571	7.6403	5.4734	1.0029
0.7	2.6999	5.3912	7.5927	5.5057	1.042
0.8	2.6899	5.3989	7.5733	5.4856	1.0072

In previous studies [29], the width of the peak corresponding to the close-packed (2 0 0) plane of the orthorhombic structure was observed to increase as Ca content increased (Fig. 1). The increase was because the interplanar distances of certain planes were close to the mean point; that is, the structure became closer to $CaMnO_3$ than $LaMnO_3$ as the Ca content increased. Therefore, the mixture had a wider reflection due to the different interplanar distances caused by the Ca atoms. This caused the crystal structure to be distorted by the volumetric strain induced by the calcium substituted at the lanthanum positions.

The crystal structure and space group by calculating the c/a parameter are shown in Table 1. The lattice distortion changed the axial symmetry from $c/a > \sqrt{2}$ to $c/a < \sqrt{2}$ without changing the *Pnma* space group. The orbitally ordered phase was designated as orthorhombic in all the studied compositions according to the refined structural results. This agreed with the t calculations, in which the tolerance factor was 0.85 and 0.825 for $LaMnO_3$ and $CaMnO_3$, respectively; both values were within the range of

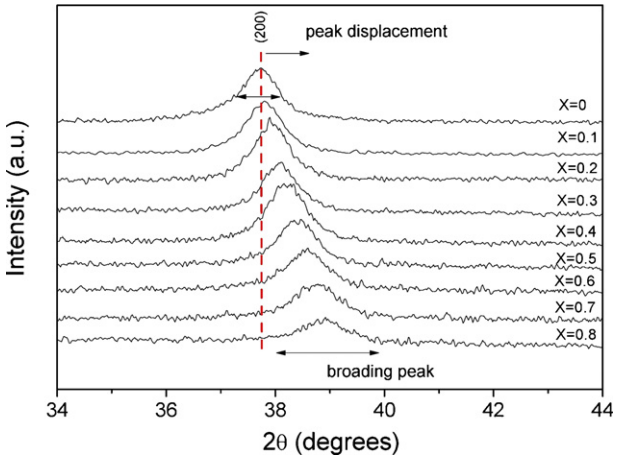

Fig. 1. X-ray diffraction patterns of $Ca_xL_{a1-x}MnO_3$ at various values of x.

the orthorhombic structure and any variations in the A site resulted in a t value between 0.825 and 0.85.

In Fig. 2, the RMS microstrain in the *Pnma* lattice of CLM with changing x content and 270 min of milling time is shown. The results confirmed that the microstrain increased with the calcium content. To study this behavior, we investigated the effect of this slight variation in the lattice parameters on the mixed ionic–electronic conductivity on CLM with $0 \leq x \leq 0.8$.

In Fig. 3a and b, the variation in the electrical resistivity of CLM as a function of temperature for several Ca^{+2} contents is shown. In general, the resistivity increased when the temperature decreased; the negative slope is typically observed in perovskite-like structures and has been predicted by Mizusaki et al. [33]. In addition, the resistivity decreased when x increased. The electrical resistivity for the synthesized materials varied from 300 Ω cm for $Ca_{0.9}La_{0.1}MnO_3$ to 10 Ω cm for $Ca_{0.8}La_{0.1}MnO_3$. Furthermore, the resistivity changed with temperature significantly when the calcium content decreased. At high temperatures, the resistivity decreased due to the increasing mobility of the ions depending on the calcium content.

The electrical resistivity of $LaMnO_3$ has been reported as approximately 10^{-4} Ω cm at room temperature and approximately 0.1 Ω cm at 973 K. The electrical conductivity of $LaMnO_3$ could be enhanced for SOFC applications by substituting a cation with a lower valence state on either the A or B sites. At a calcium content of < 50 mol%, the conductivity of $Ca_{1-x}La_xMnO_3$ increased with temperature and the maximum conductivity of $Ca_xLa_{1-x}MnO_3$ at the SOFC operating temperature occurred at 50 mol% calcium [34]. According to other authors, the CLMs synthesized by mechanical alloying could be promising materials for a wide variety of applications [1–17]. However, Fig. 3b shows that the specimen with $x = 0.8$ ($La_{0.2}Ca_{0.8}MnO_3$) had low resistivity from room temperature until close to 1400 K.

$LaMnO_3$ is a p-type semiconductor. Electronic conductivity is enhanced by substituting La^{3+} with divalent ions such as the alkaline earth dopants strontium or calcium. When a La^{3+} ion at the A site is replaced by a Ca^{2+} ion, which could occur through

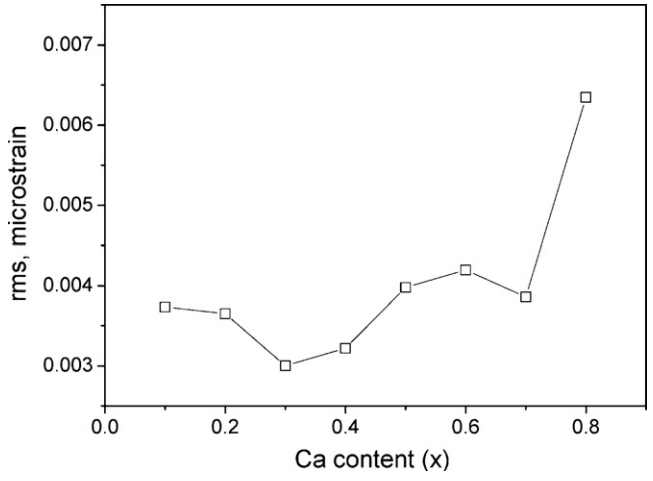

Fig. 2. Values of RMS microstrain in the *Pnma* lattice with changing calcium content (x).

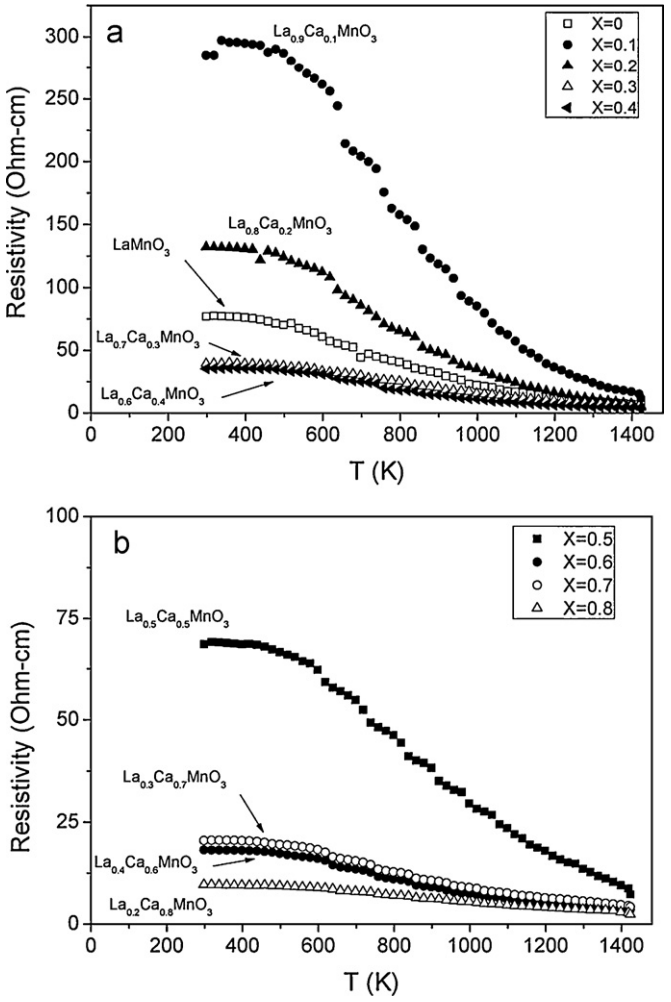

Fig. 3. Resistivity changes with the temperature for different calcium doping levels. (a) $0 \leq x \leq 0.4$ and (b) $x > 0.4$.

an increase in the oxidation number of the element in B-sites (such as Mn) or the generation of an electron hole in the B-site to maintain electroneutrality, the ionic conductivity could increase (or the resistivity could decrease) according to Eq. (2):

$$LaMnO_3 \xrightarrow{x\text{CaO}} La^{3+}_{1-x}Ca^{2+}_{x}Mn^{3+}_{1-x}Mn^{4+}_{x}O_3 \quad (2)$$

Indeed, when the doping level increases, the number of holes increases and the resistivity diminishes up to a limit given by the structure. If the value of x only results in a slight change in the lattice parameters, the structure remains the same. That is, the oxidation number of the manganese ions can only be 3+ in a $LaMnO_3$ structure; if the structure becomes more $CaMnO_3$-like, the oxidation number of the manganese ions would become 4+ to maintain charge neutrality.

We propose that the maximum ionic conductivity is obtained when the size and charge ratio of Mn^{3+}–Mn^{4+} are in a dynamic equilibrium. That is, when the oxidation number of Mn changes from 3+ to 4+, the local charge becomes mainly positive. Two such lattice points could then accommodate an O^{2-} ion. However, the O^{2-} ion would distort the lattice and an additional positive site would allow the O^{2-} ion to move and cause the latter site to be reduced. There is a maximum Mn^{3+}:Mn^{4+} ratio

at which the structure can accommodate O^{2-} ions without phase change, but the distortion would promote strain. This ratio could be found by changing the Ca content.

Fig. 4 shows the mixed ionic–electronic conductivity at various Ca levels in an Arrhenius-type graph used by Mizusaki et al. [33]. The mixed conductivity was observed to increase with temperature, particularly at high temperatures between 1000 and 1200 K that are favorable for the operation SOFCs. All manganites showed the same behavior; i.e., the curves corresponding to the different doping levels were parallel to each other. Furthermore, their first stages were in the range reported by Mizusaki [33]. At 400 K, the maximum conductivity for $Ca_{0.8}La_{0.2}MnO_3$ was approximately 0.128 S cm^{-1}. A recent study reported a conductivity of 0.139 S cm^{-1} at 873 K for the CLM obtained by mechanochemical synthesis [34], which was similar to the value reported in this work. These materials would be very useful for applications requiring high conductivities.After reviewing the work of Nagde and Bhoga [34] and conducting a thorough search for previous conductivity measurements of these materials, no conductivity data were found for the CLM synthesized by this method. The results presented in this paper would be an interesting contribution to the field of electroceramics.

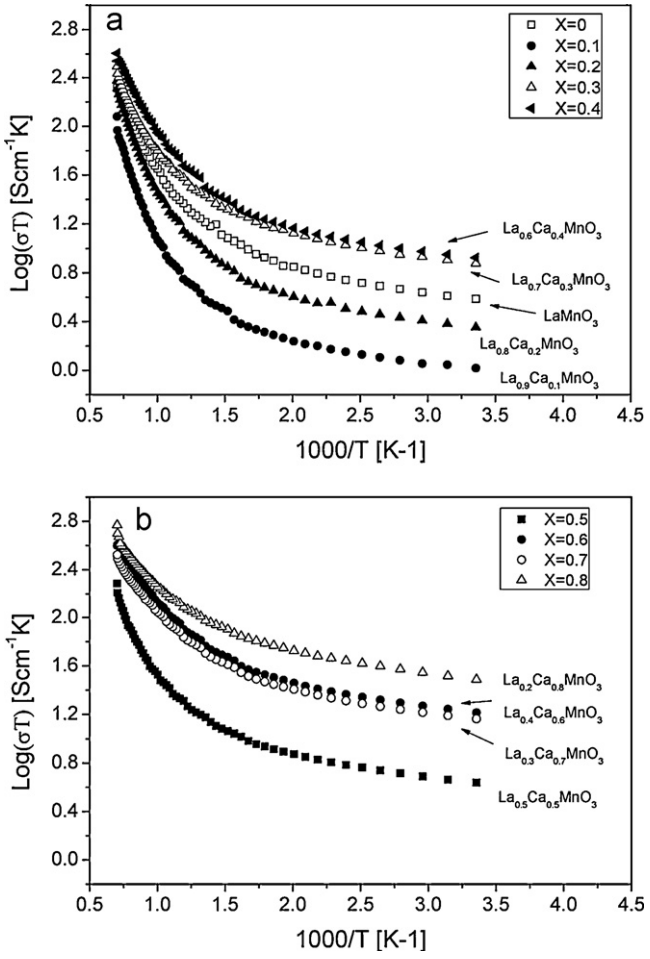

Fig. 4. The relationship between the mixed conductivity and the temperature for different calcium doping levels. (a) $0 \leq x \leq 0.4$ and (b) $x > 0.4$.

Additionally, the level of the doped calcium modified the resistivity. The mixed conductivity increased with the amount of lanthanum substitution. As seen in Fig. 5, all the curves for $La_{0.5}Ca_{0.5}MnO_3$ behaved similarly with two different stages. At low temperatures ($T < 700$ K, the first stage), the conductivity did not change significantly with the temperature. At high temperatures ($700\ K < T < 1450$ K, the second stage), the conductivity increased rapidly with the temperature, possibly due to the increase in ionic conductivity.

To obtain the activation energy to initiate conduction, each part of the curve was fitted with an Arrhenius-type equation as follows:

$$\sigma T = (\sigma T)_0 \exp\left(-\frac{E_a}{kT}\right) \quad (3)$$

As an example, the activation energy for $La_{0.5}Ca_{0.5}MnO_3$ ($x = 0.5$) was calculated by fitting the curve shown in Fig. 5. The obtained activation energies of conduction (E_a) for each stage of the curve are presented in Table 2. According to Table 2, increasing the doping level decreased the activation energy for the first stage. In the second stage, the activation energy decreased until $x = 0.4$ and then increased up to $x = 0.7$. However, the activation energy increased drastically for the manganite with $x = 0.8$. Therefore, the Mn^{3+}:Mn^{4+} ratio at maximum conductivity must be when $x = 0.8$.

Separating ion and electron conduction in these materials is a non-trivial process and requires selectively blocking electrodes, partial pressure-dependent measurements and careful modeling. We can conclude that the mixed conductivity of CLMs depends on factors such as the level of doping (x) and temperature. When the level of Ca changes, the cations still form an orthorhombic lattice. However, the octahedrons of O^{2-} become distorted, modifying the structure. The composition with the highest electrical conductivity was $La_{0.2}Ca_{0.8}MnO_3$ with a calcium concentration of 0.8; therefore, this was the best composition to manufacture the cathode of solid oxide fuel cells.

Another important property that modifies the electrical conductivity is the distortion of the perovskite structure, which

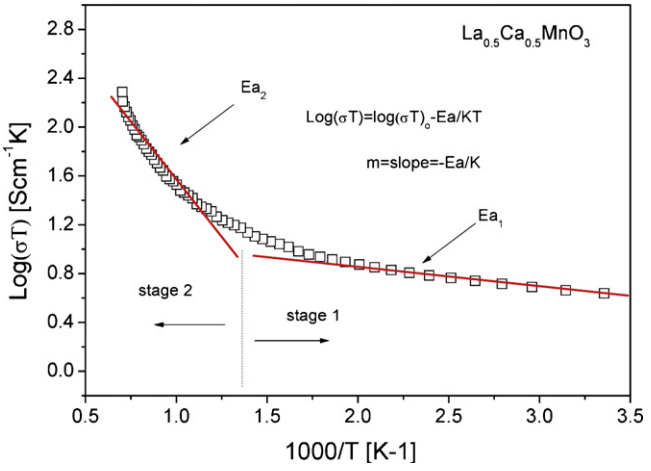

Fig. 5. An example calculation of the activation energy of the conduction process.

Table 2
Activation energies of mixed ionic–electronic conduction at the first and second stage (E_{a_1} and E_{a_2}).

Calcium level (x)	E_{a_1} (KJ/mol)	E_{a_2} (KJ/mol)
0.1	2,224.82	13,294.92
0.2	1,937.99	16,662.09
0.3	2,101.77	15,924.64
0.4	1,997.02	12,031.19
0.5	2,019.47	12,997.28
0.6	1,890.60	12,265.64
0.7	1,982.05	10,436.56
0.8	1,962.93	12,105.18

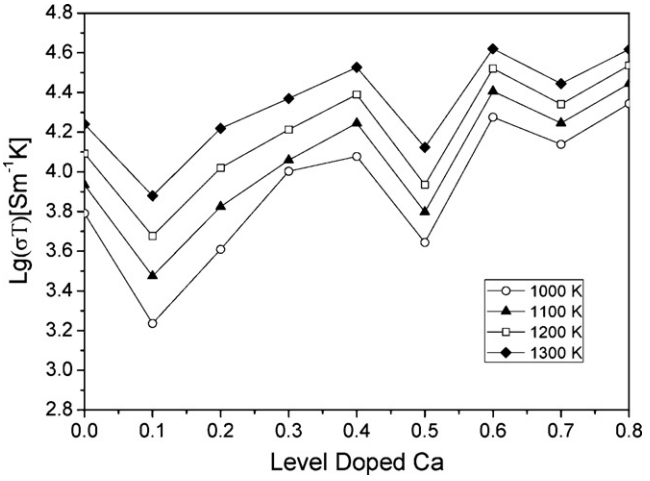

Fig. 6. The relationship between the conductivity and the level of doped calcium at various temperatures.

is affected by the amount of calcium ion in the manganite structure. It is possible for the distortion to change the conductivity of the material abruptly because each phase may have a different $\sigma(T)$ function. Fig. 6 shows that the mixed conductivity at various temperatures increased for $x > 0.1$ in $La_{1-x}Ca_xMnO_3$. For $x \approx 0.1$ and 0.5, the conductivities decreased dramatically, whereas the electrical conductivities at other levels were acceptable. This behavior could be due to the crystal structure distortion from the presence of the cations with different radii, the changes in the Mn^{3+}:Mn^{4+} ratio (which activated the mechanism known as double interchange), and the changes in the cation charges (the change from La^{3+} to Ca^{2+}).

4. Conclusions

In this work, we verified that the substitution of La^{3+} by Ca^{2+} occurred during mechanosynthesis and changed the lattice parameters, as evidenced by the displacement of the diffraction peaks. Nevertheless, the orthorhombic *Pnma* structure remained. The mixed conductivity of lanthanum doped manganite ($La_{1-x}Ca_xMnO_3$, $0 \leq x \leq 0.8$) was measured. The highest mixed conductivity was found for $x = 0.8$ which was similar to the conductivity of other perovskites and the manganites synthesized by other methods. As the calcium content increased, the activation energy for electronic conduction decreased slightly in the first stage; in the second stage, a sudden decrease in the ionic conduction was observed between $x = 0.1$ and 0.3. The mechanochemical synthesis technique could be used to prepare CLMs that could be used for different conductivity applications at high temperatures.

Acknowledgments

This project was financially supported by the National Science and Technology Council of Mexico (CONACyT) under the grant numbers 129910 and 130413. The authors are grateful for the assistance with X-ray diffraction from Adriana Tejeda Cruz from the Institute of Materials of UNAM.

References

[1] V. Markovich, G. Jung, I. Fita, D. Mogilyansky, X. Wu, A. Wisniewski, R. Puzniak, L. Titelman, L. Vradman, M. Herskowitz, G. Gorodetsky, Magnetotransport properties of ferromagnetic $LaMnO_{3+\delta}$ nano-sized crystals, J. Magn. Magn. Mater. 322 (9) (2010) 1311–1315.
[2] M. Muroi, R. Street, P.G. McCormick, Structural and magnetic properties of ultrafine $La_{0.7}Ca_{0.3}MnO_z$ powders prepared by mechanical alloying, J. Solid State Chem. 152 (2000) 503–510.
[3] N.G. Bebenin, R.I. Zainullina, V.V. Ustinov, Magnetic inhomogeneity of lanthanum manganites single crystals, J. Magn. Magn. Mater. 322 (8) (2010) 963–969.
[4] W.S. Khan, S.K. Hasanain, Resistive and magnetic behavior and their correlation in polycrystalline manganite $La_{0.55}Ca_{0.45}MnO_3$, Phys. Scr. 81 (6) (2010) 065702.
[5] A. Urushibara, Y. Morimoto, T. Arima, A. Asamitsu, G. Kido, Y. Tokura, Insulator–metal transition and giant magnetoresistance in $La_{1-x}Sr_xMnO_3$, Phys. Rev. B 51 (20) (1995) 14103–14109.
[6] J.M.D. Coey, M. Virett, Mixed-valence manganites, Adv. Phys. 48 (2) (1999) 167–293.
[7] K.P. Neupane, J.L. Cohn, H. Terashita, J.J. Neumeier, Doping dependence of polaron hopping energies in $La_{1-x}Ca_xMnO_3$ ($0 \leq x \leq 0.15$), Phys. Rev. B 74 (14) (2006) 144428.
[8] H. Taimatsu, K. Wada, H. Kaneko, Mechanism of reaction between lanthanum manganite and yttria-stabilized zirconia, J. Am. Ceram. Soc. 75 (2) (1992) 401–405.
[9] L. Kindermann, D. Das, H. Nickel, K. Hilpert, Chemical compatibility of $(La_{0.6}Ca_{0.4})_xFe_{0.8}M_{0.2}O_3$ with yttria-stabilized zirconia, J. Electrochem. Soc. 144 (2) (1997) 717–720.
[10] M. Muroi, P.G. McCormick, R. Street, Surface spin disorder and exchange bias in $La_{0.7}Ca_{0.3}MnO_3$ nanopaticles synthesised by mechanochemical processing, Rev. Adv. Mater. Sci. 5 (1) (2003) 76–81.
[11] G. Caboche, L.-C. Dufour, F. Morin, An X-ray powder diffraction study of lanthanum–strontium ferromanganites, Solid State Ionics 144 (2001) 211–222.
[12] K. Teske, H. Ullman, N. Trofimenko, Thermal analysis of transition metal and rare earth oxide system-gas interactions by a solid electrolyte-based coulometric technique, J. Therm. Anal. Calorim. 49 (3) (1997) 1211–1220.
[13] H. Ullman, N. Trokimenko, Composition, structure and transport properties of perovskite-type oxides, Solid State Ionics 119 (1999) 1–8.
[14] M. Kobayashi, R. Katsuraya, S. Kurita, M. Yamaguchi, H. Satoh, N. Kamegashira, Synthesis and crystal structure of (Ca, R)(Mn, Ti)O_3 (R, rare earth), J. Alloys Compd. 408 (412) (2006) 1173–1176.
[15] D. Flahaut, T. Mihara, R. Funahashi, N. Nabeshima, K. Lee, H. Ohta, K. Koumoto, Thermoelectrical properties of A-site substituted $Ca_{1-x}Re_xMnO_3$ system, Appl. Phys. 100 (2006) 084911.
[16] R. Von Helmolt, J. Wecker, B. Holzapfel, L. Schultz, K. Samwer, Giant negative magnetoresistance in perovskitelike $La_{2/3}Ba_{1/3}MnO_x$ ferromagnetic films, Phys. Rev. Lett. 71 (14) (1993) 2331–2333.

[17] S. Jin, T.H. Tiefel, M. McCormack, R.A. Fastnacht, R. Ramesh, L.H. Chen, Thousandfold change in resistivity in magnetoresistive La–Ca–Mn–O films, Science 264 (5157) (1994) 413–415.
[18] F. Padella, C. Alvani, A. Barbera, G. Nenas, R. Liberatore, F. Varsano, Mechanosynthesis and process characterization of nanostructured manganese ferrite, Mater. Chem. Phys. 90 (2005) 172–177.
[19] H. Taguchi, D. Matsuda, M. Nagano, K. Tanihata, Y. Miyamoto, Synthesis of perovskite-type $(La_{1-x}Sr_x)MnO_3$ ($O \leq x \leq 0.3$) at low temperature, J. Am. Ceram. Soc. 75 (1) (1992) 201–202.
[20] R.D. Sanchez, J. Rivas, C. Vazquez-Vazquez, A. Lopez-Quintela, M.T. Causa, M. Tovar, S. Oseroff, Giant magnetoresistance in fine particle of $La_{0.67}Mn_{0.33}O_3$ sinthesized at low temperatures, Appl. Phys. Lett. 68 (1) (1996) 134–136.
[21] V.M. Browning, R.M. Stroud, W.W. Fuller-Mora, J.M. Byers, M.S. Osofsky, D.L. Knies, K.S. Grabowski, D. Koller, J. Kim, D.B. Chrisey, J.S. Horwitz, Magnetic and transport properties of radiation damaged $La_{0.7}Ca_{0.3}MnO_3$ thin films, J. Appl. Phys. 83 (1998) 7070–7072.
[22] A. Asamitsu, Y. Murimoto, R. Kumai, Y. Tomioka, Magnetostructural phase transitions in $La_{1-x}Sr_xMnO_3$ with controlled carrier density, Phys. Rev. B 54 (3) (1996) 1716–1723.
[23] Suryanarayana, Mechanical alloying and milling, Prog. Mater. Sci. 46 (2001) 1–184.
[24] W. Tae Jeong, J. Hyun Joo, K. Sub Lee, Synthesis of spinel $LiMn_2O_4$ powders for lithium ion battery by mechanical alloying of Li_2O_2 and Mn_2O_3, J. Alloys Compd. 358 (2003) 294–301.
[25] E. Gaffet, F. Bernard, J.C. Niepce, F. Charlot, C. Gras, G. Le Caër, J.L. Guichard, P. Delcroix, A. Mocellin, O. Tillement E, Some recent developments in mechanical activation and mechanosynthesis, J. Mater. Chem. 9 (1) (1999) 305–314.
[26] Z. Jin, W. Tang, J. Zhang, Y. Du, Giant magnetoresistance in mechanical alloyed $La_{0.7}Sr_{0.06}Ca_{0.24}MnO_3$ perovskite, J. Magn. Magn. Mater. 187 (1998) 237–241.
[27] A.M. Bolarín, F. Sánchez, S. Palomares, J.A. Aguilar, G. Torres, Synthesis of calcium doped lanthanum manganite by mechanosynthesis, J. Alloys Compd. 436 (2007) 335–340.
[28] A.M. Bolarín, F. Sánchez, A. Ponce, E.E. Martinez, Mechanosynthesis of lanthanum manganite, Mater. Sci. Eng. 454 (455) (2007) 69–74.
[29] I.A. Lira, F. Sanchez, C.A. Cortés, A.M. Bolarin, Crystal structure analysis of calcium-doped lanthanum manganites prepared by mechanosynthesis, J. Am. Ceram. Soc. 93 (10) (2010) 3474–3477.
[30] Q. Zhang, F. Saito, Mechanochemical synthesis of $LaMnO_3$ from La_2O_3 and Mn_2O_3 powders, J. Alloys Compd. 297 (1–2) (2000) 99–103.
[31] L. Lutterotti, S. Matthies, H.R. Wenk, MAUD. A friendly Java program for material analysis using diffraction, 2114-5, IUCr: Newsletter of the CPD, 1999.
[32] Z. Zhan, S.I. Lee, Thin film solid oxide fuel cells with copper cermet anodes, J. Power Sources 195 (2010) 3494–3497.
[33] J. Mizusaki, Y. Yonemura, H. Kamata, K. Ohyama, N. Mori, H. Takai, H. Tagawa, M. Dokiya, K. Naraya, T. Sasamoto, H. Inaba, T. Hashimoto, Electronic conductivity, Seebeck coefficient, defect and electronic structure of nonstoichiometric $La_{1-x}Sr_xMnO_3$, Solid State Ionics 132 (2000) 167–180.
[34] K.R. Nagde, S.S. Bhoga, Study of mechanochemically prepared nanocrystalline $La_{0.8}Sr_{0.2}MnO_3$, Ionics 16 (2010) 361–370.